AWARD NUMBER: W81XWH-16-1-0314

TITLE: Discovery and characterization of PRCAT47: A novel prostate lineage and cancer specific long non-coding RNA

PRINCIPAL INVESTIGATOR: Rohit Mehra, M.D.

CONTRACTING ORGANIZATION: Regents of the University of Michigan
Ann Arbor, MI 48109

REPORT DATE: July 2018

TYPE OF REPORT: Annual

PREPARED FOR: U.S. Army Medical Research and Materiel Command
Fort Detrick, Maryland 21702-5012

REPORT DOCUMENTATION PAGE

Form Approved
OMB No. 0704-0188

1. REPORT DATE	2. REPORT TYPE	3. DATES COVERED
July 2018	Annual	1 July 2017 - 30 June 2018

4. TITLE AND SUBTITLE

Discovery and characterization of PRCAT47: A novel prostate lineage and cancer specific long non-coding RNA

5a. CONTRACT NUMBER

5b. GRANT NUMBER
W81XWH-16-1-0314

5c. PROGRAM ELEMENT NUMBER

6. AUTHOR(S)

Rohit Mehra, M.D.

E-Mail: mrohit@med.umich.edu

5d. PROJECT NUMBER

5e. TASK NUMBER

5f. WORK UNIT NUMBER

7. PERFORMING ORGANIZATION NAME(S) AND ADDRESS(ES)

Regents of the University of
Michigan
Ann Arbor, MI 48109-1340

8. PERFORMING ORGANIZATION REPORT NUMBER

9. SPONSORING / MONITORING AGENCY NAME(S) AND ADDRESS(ES)

U.S. Army Medical Research and Materiel Command
Fort Detrick, Maryland 21702-5012

10. SPONSOR/MONITOR'S ACRONYM(S)

11. SPONSOR/MONITOR'S REPORT NUMBER(S)

12. DISTRIBUTION / AVAILABILITY STATEMENT

Approved for Public Release; Distribution Unlimited

13. SUPPLEMENTARY NOTES

14. ABSTRACT

The overall goal of this project is to characterize the functioning mechanism, utility and therapeutic potential of the biomarker PRCAT47 in prostate cancer. During this second period, we investigated the regulatory effect of PRCAT47 on androgen receptor (AR)transcript stability. We also interrogated the role of PRCAT47 in regulating HuR/TIAR-targeted mRNAs. Utilizing a novel RNA in situ hybridization technology optimized within the first period which allows us to assess PRCAT47 expression in prostate tissues, we have not evaluated PRCAT47 expression in prostate cancer tissue microarrays by RNA-ISH and demonstrate an association with prostate cancer progression. Finally, we also assessed the therapeutic potential of PRCAT47 using cell line models and patient derived organoid cultures.

15. SUBJECT TERMS

Prostate cancer; long non-coding RNA; PRCAT47

16. SECURITY CLASSIFICATION OF:			17. LIMITATION OF ABSTRACT	18. NUMBER OF PAGES	19a. NAME OF RESPONSIBLE PERSON
a. REPORT	b. ABSTRACT	c. THIS PAGE			USAMRMC
Unclassified	Unclassified	Unclassified	Unclassified	22	19b. TELEPHONE NUMBER *(include area code)*

Table of Contents

Introduction

Long non-coding RNAs (lncRNA) are a class of transcripts that are longer than 200 nucleotides in length, and do not code for proteins. Like mRNAs, these transcripts undergo polyadenylation, and their expressions are regulated by epigenetic modifications. Previously, our laboratory performed a comprehensive analysis of long non-coding RNAs in human transcriptome[1]. This study highlighted the existence of tissue lineage-specific lncRNAs, cancer-associated lncRNAs, and conserved lncRNAs. Although hundreds of lncRNAs have suggested oncogenic roles or tumor repressive roles, a limited number of them have been studied in details regarding their functions in cancer development.

Prostate cancer is the most common type of cancer in American men. In 2018, it is estimated that 164,690 new cases of prostate cancer would be diagnosed, and that 29,430 deaths would be caused by prostate cancer [2]. Androgen receptor (AR) signaling plays a central role in normal prostate development, as well as in prostate cancer progression[3]. Thus, most of the patients with local or regional prostate cancer could be hypothetically cured by androgen deprivation therapy, with a ~100% 5-year survival rate. However, it is well known that some patients develop prostate cancer which can be aggressive locally and metastasize; the 5-year survival rate drops to ~29% in such patients[4,5]. Since this state of disease generally does not response to androgen deprivation therapy, it is referred to as castration resistant prostate cancer (CRPC). Multiple pathological drivers contributing to CRPC have been identified, including AR mutation/amplification, AR-target gene activation by other receptors, etc[6-8]. However, most of these studies have previously focused on protein-coding genes, while the potential role of lncRNAs has not been thoroughly investigated. Few lncRNAs have been demonstrated to have oncogenic roles, or to serve as prognostic markers in prostate cancer. Examples of these lncRNAs include PCA3, which is used to determine risk of prostate cancer, and SchLAP1, which is known to be associated with poor outcome in prostate cancer.

Considering the critical function of AR signaling in primary clinically localized prostate cancer and castration resistant metastatic prostate cancer, as well as a lack of functional study of lncRNAs within this context, our laboratory initiated a study to comprehensively profile AR-regulated lncRNAs that are prostate lineage-specific and associated with prostate cancer progression. This study prioritized a lncRNA candidate, PRCAT47, which is directly regulated by AR. Expression of this lncRNA is prostate lineage specific, and is higher in prostate cancer tissue (compared to benign prostate). Further characterization of this lncRNA has demonstrated PRCAT47 depletion inhibits AR-positive prostate cancer cell growth, and results in increased apoptosis. Interestingly, we also discovered that loss of PRCAT47 resulted in suppressed AR signaling, which was reflected by decreased AR target gene expression, reporter gene assay, as well as Gene Set Enrichment Analysis. To discover the functioning mechanisms behind this phenotype, we performed Mass Spectrometry analysis to identify PRCAT47-binding proteins. Two proteins among the proteins identified, HuR (ELAV1) and TIAR, are of special interest, since they have also been reported to mediate AR transcript stability[9].

In this project, we sought to further explore the mechanism through which PRCAT47 is involved in AR signaling, to evaluate the potential of PRACT47 as a diagnostic marker, and to test whether PRCAT47 serves as a therapeutic target.

Keywords

Prostate cancer; long non-coding RNA; PRCAT47

Accomplishments

We hypothesized that PRCAT47 mediates the development and progression of prostate cancer by regulating androgen receptor signaling, and thus can be developed into a promising biomarker and therapeutic target. To test this hypothesis, we performed a series of experiments during this research cycle, aiming to answer three specific questions:

(1) What is the functioning mechanism behind the PRCAT47-AR positive feedback loop?
(2) Does PRCAT47 serve as a diagnostic marker?
(3) Does PRCAT47 have therapeutic potential in treatment of castration resistant prostate cancer?

Outline of the accomplishments finished in this research cycle are listed below:

1. **Using BrU-Seq and BrUChase-seq technology to understand the regulatory effect of PRCAT47 on AR transcript stability.**

   (1) Analysis of AR transcript synthesis and stability by BrU-PCR and BrUChse-PCR.
   (2) BrU-Seq and BrUChase-Seq analysis of transcript synthesis and stability in MDA-PCa-2b cells.

2. **Using RIP-PCR technology to study the involvement of PRACT47-binding protein, HuR, in PRACT47-regulation on AR transcript.**

3. **Investigating the role of PRCAT47 in regulating HuR/TIAR-targeted mRNAs.**

   (1) Identification of HuR- and TIAR- targeted transcripts in MDA-PCa-2b and LNCaP cells using RIP-Seq technology.
   (2) Identification of transcript targets that are directly regulated by HuR and TIAR.
   (3) Assessing the influence of PRCAT47 loss on direct HuR/TIAR target.

4. **Evaluation of PRCAT47 expression in prostate cancer tissue microarrays (TMAs) by ISH**

5. **Evaluate the biomarker potential of PRCAT47 by measuring the expression in urine samples obtained from patients with prostate cancer**

6. **Interrogating the therapeutic potential of PRCAT47 using cell line models and patient derived organoid cultures.**

   (1) Interrogating PRCAT47 expression in a series of patient-derived xenografts.
   (2) Evaluating *in-vivo* free-uptake efficacy of antisense oligonucleotides targeting PRCAT47.
   (3) Generation of cell-line derived xenograft in mice using MDA-PCa-2b cells.

For each specific experiments listed above, a detailed description of methods, activities, significant results, conclusion, and discussion are as follows.

1. Using BrU-Seq and BrUChase-seq technology to understand the regulatory effect of PRCAT47 on AR transcript.

Methods and activities:

In the previous research cycle, to answer the question how PRCAT47 affected AR at transcript level, we measured the stability of AR mRNA in cells depleted of PRCAT47, following treatment with actinomycin D (an inhibitor of mRNA transcription). We observed a shortened AR mRNA half-life following PRCAT47 loss, and thus concluded that PRCAT47 exerted post-transcriptional regulatory effect on AR transcript. Nonetheless, this observation did not exclude the possibility that PRCAT47 also regulates AR at transcriptional level. To profile both the synthesis rate and degradation rate of AR transcript, we employed BrU-Seq and BrUChase-Seq technology[10], upon PRCAT47 knockdown. Briefly, for BrU-Seq, cells were treated with siRNA targeting PRCAT47 or si-NT for 72 hours, and then pulse-labeled using bromouridine for 30 minutes. Newly synthesized transcripts were then labeled with bromouridine. For BrUChase-Seq, after pulse-labeling, cells were maintained in normal chase media (with normal uridine) for 6 hours and then bromouridine-labeled RNA was extracted. This RNA population represented the synthesized transcripts remained after 6-hour degradation. Following this pipeline, we first performed BrU/BrUChase-PCR analysis, and then performed BrU/BrUChase-Seq, in MDA-PCa-2b cells.

Results and conclusion:

(1) Analysis of AR transcript synthesis and stability by BrU-PCR and BrUChase-PCR.

BrU-PCR and BrUChase-PCR assays were performed on PRCAT47 transcript, and on AR transcript, following treatment of PRCAT47 siRNA. As a positive control, upon si-PRCAT47 treatment, we observed attenuated expression levels of both newly-synthesized PRCAT47 transcripts and PRCAT47 transcripts remained after degradation (Figure 1, Left). Interestingly, for AR transcript, the synthesis rate remained similar, while the transcripts remained after degradation decreased drastically. This result suggested that the synthesis rate of AR transcript remained the same upon PRCAT47 loss, while the stability of the transcript decreased (Figure 1, Right).

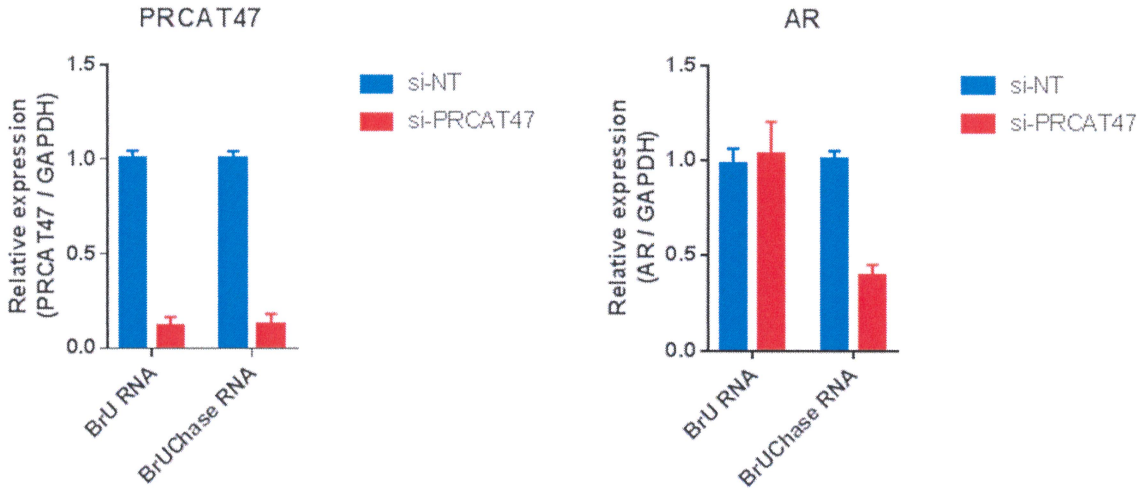

Figure 1: BrU-PCR and BrUChase-PCR results for PRCAT47 transcript (Left) and for AR transcript (Right) in MDA-PCa-2b cells, following treatment of siRNA targeting PRCAT47.

(2) BrU-Seq and BrUChase-Seq analysis of transcript synthesis and stability in MDA-PCa-2b cells.

Based on the observation from BrU-PCR and BrUChase-PCR analysis, we further performed BrU-Seq and BrUChase-Seq analysis (Figure 2). Interestingly, at the AR locus, following PRCAT47 knockdown, we observed no changes on transcript synthesis, while there was a decrease on transcript stability, preferentially at the 3'UTR region of AR. This result echoed our previous observation from qPCR analysis, and demonstrated the involvement of AR 3'UTR in mediating transcript stability.

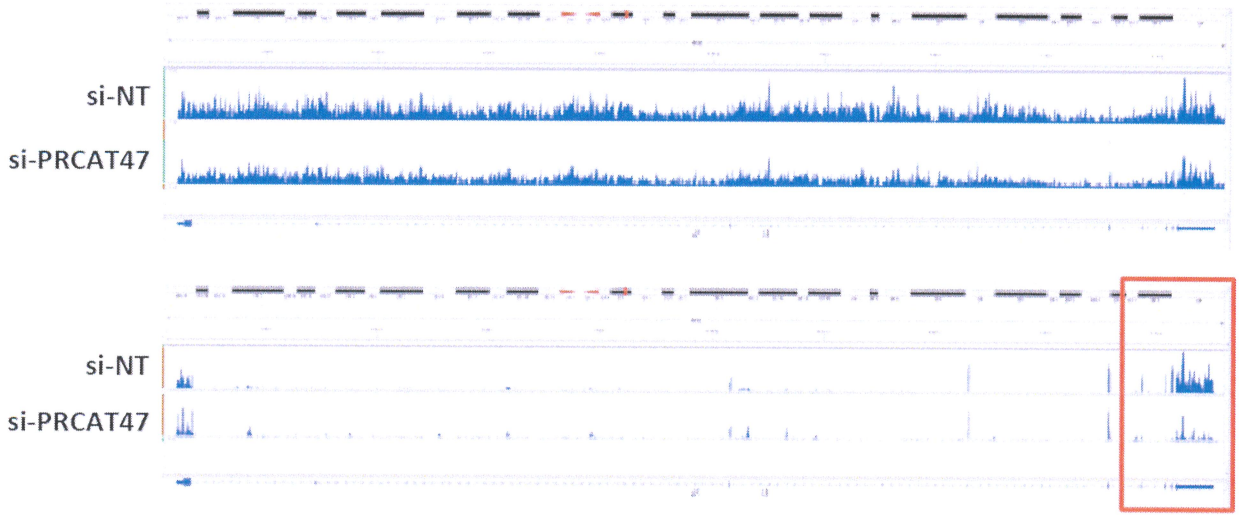

Figure 2: BrU-Seq (Top) and BrUChase-Seq tracks (Bottom) at AR genomic locus from MDA-PCa-2b cells.

Discussion:

The results from BrU-Seq and BrUChase-Seq experiment, together with results gained from last research cycle, indicated that PRCAT47 regulates AR transcript stability at post-transcriptional level, not transcriptional level. This observation highlights the potential involvement of AR 3'UTR in this regulation process. Interestingly, within the PRCAT47-binding protein list we identified previously from Mass-Spectrometry, two high-ranked proteins, HuR (ELAV1) and TIAR, have previously been reported to bind with AR 3'UTR, and regulates AR transcript stability. Therefore, we next sought to study the involvement of PRACT47-binding proteins, HuR and TIAR, in PRACT47-regulation on AR transcript.

2. Using RIP-qPCR technology to study the involvement of PRACT47-binding protein, HuR, in PRACT47-regulation on AR transcript.

Methods and activities:

Given the potential involvement of HuR in PRCAT47-regulation on AR transcript, we performed RNA immunoprecipitation (RIP)-qPCR experiments to validate binding between HuR and AR mRNA. HuR- specific antibody was used to immuno-precipitate RNAs associated with HuR protein. qPCR analysis was then performed using AR-specific primers. Primers targeting Actin, a known HuR binding protein, was used as positive control. IgG serves as negative control for antibody against HuR protein.

To further test whether PRCAT47 loss affect HuR-AR mRNA binding, we performed RIP-qPCR experiment after PRCAT47 depletion. Binding affinity between HuR and AR transcript was tested by qPCR analysis.

Results and conclusion:

As shown in Figure 3, in MDA-PCa-2b cells, we observed a strong binding between HuR protein and a positive control mRNA, Actin (Figure 3, right panel). This result indicated a successful RIP experiment. Meanwhile, AR transcripts were also significantly bound by HuR (Figure 3, left panel). Interestingly, following PRACT47 knockdown, HuR-AR transcript binding decreased significantly, while binding between HuR and Actin mRNA did not change much. This result suggested that PRACT47 loss resulted in decreased HuR binding to AR transcript.

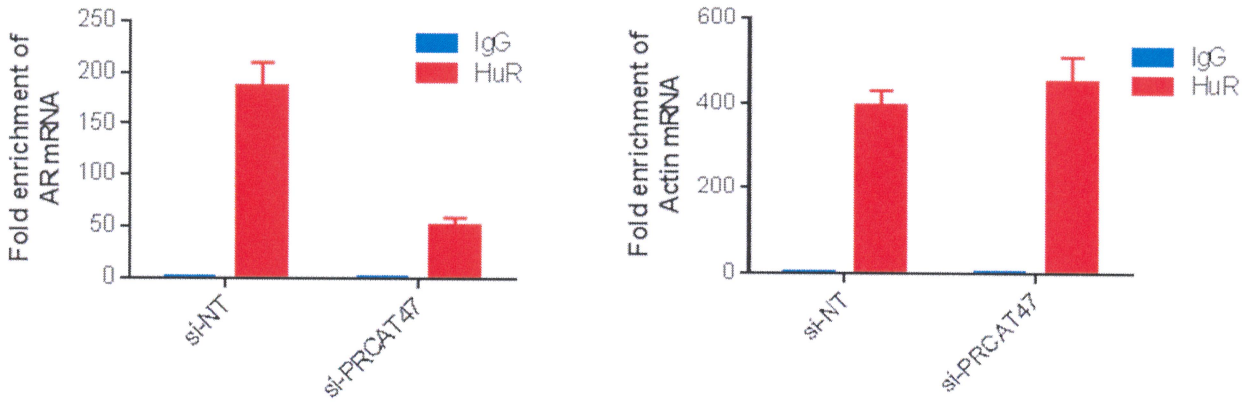

Figure 3: Fold enrichment of AR mRNA (Left) and Actin mRNA (Right) measured by qPCR analysis following RNA immunoprecipitation by HuR antibody or IgG. RIP experiment was performed in MDA-PCa-2b cells, following transfection of non-targeting siRNA or siRNA targeting PRCAT47.

Discussion:

Published studies have uncovered the role of HuR in mediating AR transcript stability[9]. This role was realized by HuR binding to the AU-rich region located at AR 3'UTR. The binding was validated in our study by RIP-qPCR assay, and this binding affinity was attenuated upon PRCAT47 depletion. Our result suggests that PRACT47 mediates HuR-stabilization of AR transcript. Loss of PRACT47 decreases HuR binding to AR mRNA, thus affecting AR transcript stability.

3. Investigation of the role of PRCAT47 in regulating HuR/TIAR-targeted mRNAs.

Methods and activities:

During the last reported research cycle, we profiled the global gene expression change upon knockdown of HuR and TIAR in MDA-PCa-2b and LNCaP cells, using non-targeting siRNA as a control. We further performed Gene Set Enrichment Analysis and discovered that androgen receptor signaling genes were enriched in HuR- and TIAR- regulated gene sets. To further identify direct mRNA targets of HuR protein and TIAR protein, we performed RNA immunoprecipitation (RIP)-Seq experiments in this research cycle. Briefly, we used HuR- and TIAR- specific antibodies to immuno-precipitate HuR- and TIAR- bound RNAs, followed by high throughput sequencing. IgG was used as negative control. After identification of direct HuR- and TIAR- targets, we further interrogated the overlap between these targets and previously identified PRCAT47-regulated genes.

Results and conclusion:

(1) Identification of HuR- and TIAR- targeted transcripts in MDA-PCa-2b and LNCaP cells using RIP-Seq technology.

As shown in Figure 4, in MDA-PCa-2b cells, a total of 11886 transcripts were identified as HuR-binding transcripts, while in LNCaP cells, 11227 transcripts bound to HuR. Overall, 9907 transcripts were overlapped between the two types of cells, suggesting a highly reproducible HuR-binding transcriptome in AR-positive prostate cancer cells. Similarly, TIAR protein associated with 9658 transcripts in both MDA-PCa-2b and LNCaP cells. Importantly, both AR and PRCAT47 were identified as HuR-binding transcript and TIAR-binding transcript across these two cell lines.

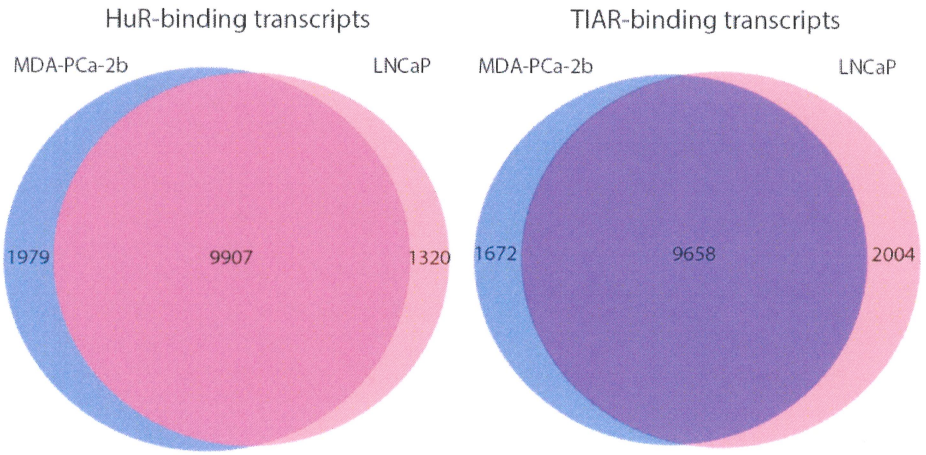

Figure 4: Venn Diagrams indicating number of transcripts bound by HuR and TIAR in MDA-PCa-2b cells and LNCaP cells.

(2) Identifications of transcript targets that are directly regulated by HuR and TIAR.

RIP-Seq technique allowed us to identify a large amount of transcripts that bind with HuR and TIAR, we thus wondered how many of them are directly regulated following HuR/TIAR loss. To achieve this goal, we leveraged the gene expression profiling data obtained during the last research cycle, and queried the overlapping gene sets between HuR/TIAR-binding transcripts and genes affected upon HuR/TIAR loss.

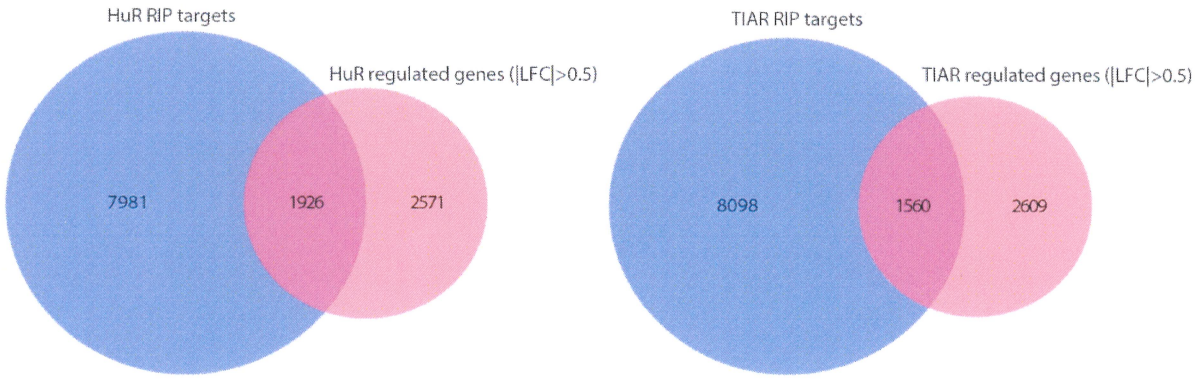

Figure 5: Venn Diagrams indicating overlap between transcripts bound by HuR (or TIAR), and transcripts regulated by HuR (or TIAR).

Within transcripts significantly regulated by HuR ($|LFC| > 0.5$, adjusted P value < 0.01), nearly half of them are direct HuR-binding targets (Figure 5, Left). Therefore, ~50% of the observed gene alterations are likely to be mediated directly by HuR-mRNA interaction. TIAR-regulated genes follow the same trend with HuR targets (Figure 5, Right). It is also of notice that expression levels of the majority of HuR/TIAR-bound mRNAs did not change upon HuR/TIAR knockdown. This might be explained by the fact that HuR and TIAR are non-specific RNA-binding proteins that recognize a broad range of RNA targets. It is, therefore, of importance to find out their functional downstream targets under different pathological conditions. In our current cell line models, we defined the "direct HuR/TIAR targets" as HuR/TIAR-bound transcripts that have altered expression level following HuR/TIAR loss (indicated by the insect portions of Venn Diagrams in Figure 5).

(3) Assessing the effect of PRCAT47 loss on HuR/TIAR targets.

To understand whether HuR and TIAR are involved in PRACT47 regulation on its target genes, we further intersected the gene expression data obtained after PRCAT47 knockdown with the list of direct HuR and TIAR targets. Interestingly, a significant portion (~25%, using |LFC| > 0.5) of PRCAT47-regulated transcriptome is direct HuR targets (Figure 6a). Loss of PRCAT47 and loss of HuR induces similar expression changes in this set of genes (Figure 6c). Moreover, AR is within this gene set. Similar overlap exits between PRACT47- and TIAR- regulated genes (Figure 6b).

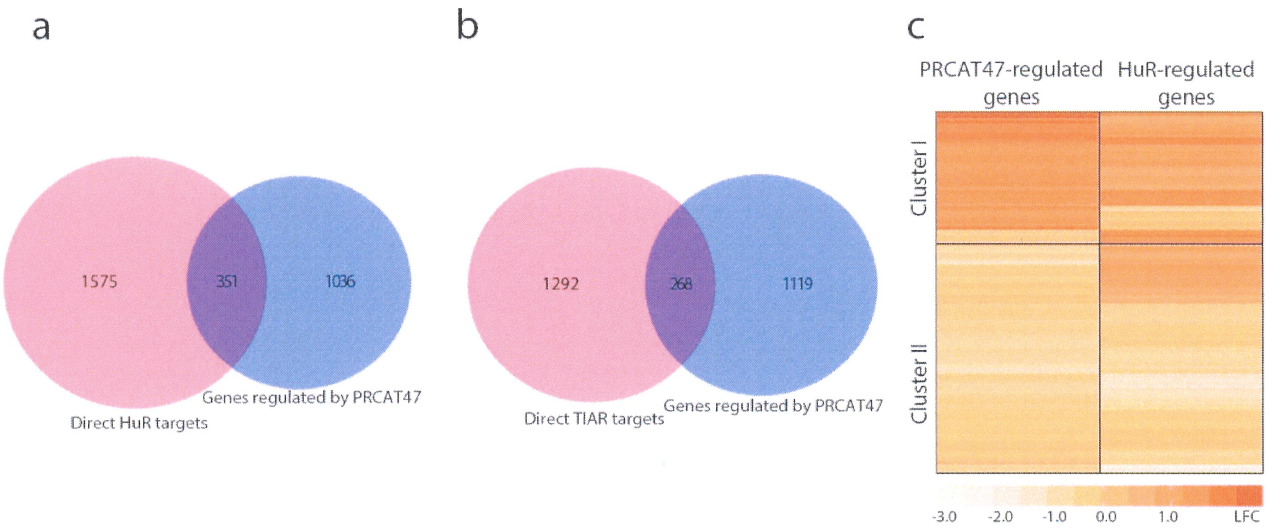

Figure 6: Overlap between PRCAT47-regulated genes and direct HuR/TIAR targets. a, Venn Diagram indicating the overlapped gene number between direct HuR targets and PRCAT47-responsive targets. b, Venn Diagram indicating the overlapped gene number between direct TIAR targets and PRCAT47-responsive targets. c, a heatmap representing the degree of gene expression change (indicated by LFC) of PRCAT47-responsive HuR targets following loss of PRCAT47 or HuR.

Discussion:

As part of the effort to dissect functioning mechanisms of PRCAT47, we have comprehensively studied the roles of PRCAT47 in regulating direct HuR and TIAR targets. We focused on HuR and TIAR proteins because they were identified as top PRCAT47-interacting partners from Mass-Spectrometry analysis following RNA-immunoprecipitation. Both HuR and TIAR are mRNA-binding proteins that mediate mRNA stability and transportation between nuclei-cytoplasm cellular compartments. In the reported research cycle, we first profiled the HuR/TIAR associated RNA species using RIP-Seq. We then overlaid this data with HuR/TIAR-regulated gene sets identified from last research cycle. This analysis enabled the identification of direct HuR/TIAR targets. Furthermore, to delineate the involvement of PRCAT47 in modulating direct HuR/TIAR targets, we further queried the overlap between these targets and PRCAT47-responsive gene sets. Throughout this process, we found that the PRCAT47 loss affects the expression of ~20%

HuR/TIAR targets. Interestingly, expression changes of these targets are moving in the same direction between PRCAT47-loss condition and HuR-loss condition, suggesting that the PRCAT47-HuR interaction is essential for maintaining expression levels of certain mRNA transcripts. Moreover, we observed AR mRNA as one of these transcripts, which echoes our previous observations of PRCAT47- and HuR- regulation on AR stability.

4. Evaluation of PRCAT47 expression in prostate cancer tissue microarrays (TMAs) by ISH

Methods and activities:

FFPE sections were baked at 60°C for one hour. Tissues were deparaffinized by immersing in xylene twice for five minutes each with periodic agitation. The slides were immersed in 100% ethanol twice for one minute each with periodic agitation and then air-dried for five minutes. After a series of pretreatment steps, the cells were permeabilized using Protease Plus to allow probes access to the RNA target. Hybridization of the probes to the RNA targets was performed by incubation in the HybEZ™ Oven for two hours at 40°C. After two washes, the slides were processed for standard signal amplification steps. Chromogenic detection was performed using DAB followed by counterstaining with 50% Gill's Hematoxylin I (Fisher, 26801-01).

Slides were examined for PRCAT47 ISH signals in morphologically intact cells. PRCAT47 ISH signal was identified as brown, punctate dots, and expression level was scored as follows: 0 = no staining or less than 1 dot per 10 cells, 1 =1 to 3 dots per cell, 2 =4 to 9 dots per cell (few or no dot clusters), 3 =10 to 15 dots per cell (less than 10% in dot clusters), and 4 = greater than 15 dots per cell (more than 10% in dot clusters). A cumulative ISH product score was calculated for each evaluable tissue core as the sum of the individual products of the expression level (0 to 4) and percentage of cells (0 to 100) (i.e., [A%× 0] + [B%× 1] +[C%× 2] + [D% × 3] + [E% × 4]; total range =0 to 400). For each tissue sample, the ISH product score was averaged across evaluable TMA tissue cores.

Results and conclusion:

We have performed RNA-ISH expression of PRCAT47 in a spectrum of tissues representing benign prostatic tissue (n = 11), clinically localized prostate cancer (n = 85, with associated long-term clinical follow-up information) and metastatic hormone refractory prostate cancer (n = 37, from a unique cohort of "rapid autopsy" patients at University of Michigan). Representative PRCAT47 staining is shown for benign prostate, localized, and metastatic prostate cancer tissue. Bar plot represents mean PRCAT47 expression scores across benign, localized, and metastatic tissues, with vertical bars indicating bootstrapped 95% CI of the means. Significance was calculated by a Kruskal-Wallis rank sum test.

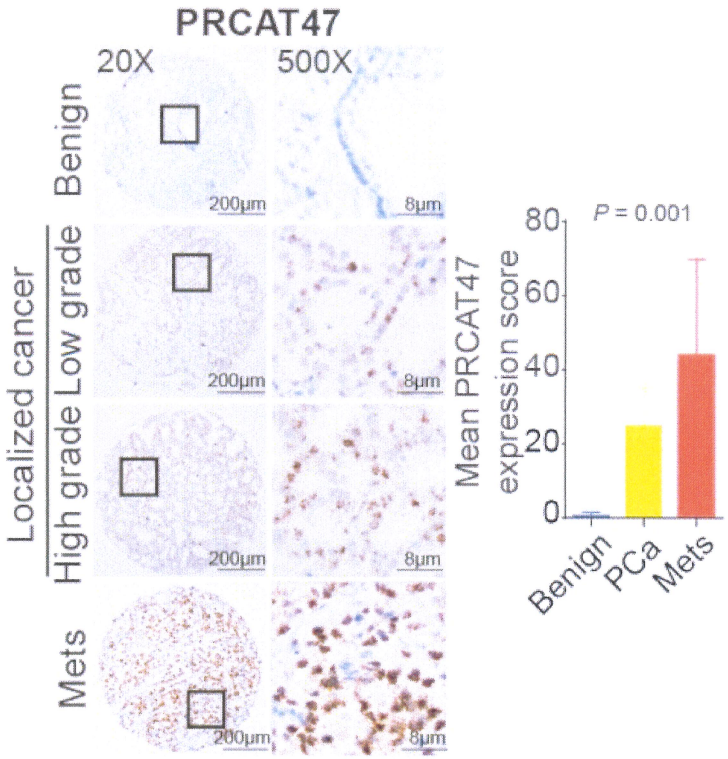

Figure 7: Evaluation of PRCAT47 expression across different grades of prostate cancer samples. Left, representative PRCAT47 ISH images of benign prostate, localized prostate cancer, and metastasis prostate cancer samples. Right, quantified PRCAT47 expression scores in prostate cancer sample groups of various grades.

Discussion:

Taking the 133 tissues as independent units, the PRCAT47 expression level was significantly higher in localized cancer and metastatic disease, compared with benign prostate. This result is in accord with our previous observation obtained from analyzing RNA-seq data.

5. Evaluate the biomarker potential of PRCAT47 by measuring the expression in urine samples obtained from patients with prostate cancer.

Methods and activities:

In this aim, we sought to investigate the potential of PRCAT47 as a biomarker using non-invasive platforms (urine). We plan to assess the expression of PRCAT47 and its association with clinical parameters. During the reported research cycle, we developed a platform to quantify PRCAT47 expression in urine samples. Patient urine samples were collected via the University of Michigan

urology clinic. Total urine RNA was extracted using Thermo Fisher MagMAX mirVana RNA isolation kit, a magnetic beads-based RNA isolation system that specifically designed for total urine RNA isolation. RNA quality was checked on the Agilent Bioanalyzer. We then utilized Thermo Fisher Next Generation Sequencing-based RNA screening assay to quantify expression level of PRCAT47 transcript. To eliminate potential bias caused by the targeted amplicons, we designed two sets of probes spanning exons 2 to 4 of the PRCAT47 transcript.

Results and Plan:

We have now established a PRCAT47 detection platform. During the next research cycle, we will quantify the diagnostic potential of PRCAT47 by calculating the likelihood ratio and the area under the receiver-operating-characteristic (ROC) curve (AUC). We will further compare the ROC curves between PRCAT47 and other known cancer biomarkers on the same collection of urine samples.

6. Interrogating the therapeutic potential of PRCAT47 using cell line models and patient derived organoid cultures.

Methods and activities:

During the last research cycle, we systematically characterized the therapeutic potential of PRCAT47 using clinical grade anti-sense oligonucleotides (ASOs) in *in-vitro* cell line models. On-target effects of ASOs were evaluated following transfections. We observed similar gene expression profile change between ASO treatment and siRNA treatment conditions. Furthermore, phenotypic effects, including retarded tumor growth, were also observed post ASO treatment. A potential problem limiting the clinically translation of ASOs is their ability to be up-taken freely in cells. Therefore, we further tested the free-uptake efficacy of the designed ASOs, and chose the ASO with high free-uptake efficacy and low toxicity to use for *in vivo* experiments.

In the current research cycle, we focused on searching for proper patient-derived xenografts and cell line derived xenografts to perform ASO subcutaneous treatment *in vivo*. Pilot experiments were performed to set up *in vivo* tumor models and to test ASO free-uptake efficacy in tumors.

Results and conclusion:

(1) Interrogating PRCAT47 expression in a series of patient-derived xenografts.

To find a patient-derived xenograft with relatively high PRCAT47 expression, we queried PRCAT47 expression using the RNA-Seq data of a series of patient-derived xenografts. We found that PRCAT47 was highly expressed in MDA-146-12, MDA-117-9, and MDA-79 cell lines.

Within these xenografts, only xenograft MDA-146-12 was available in lab, therefore, we used this xenograft for the *in-vivo* treatment of ASOs.

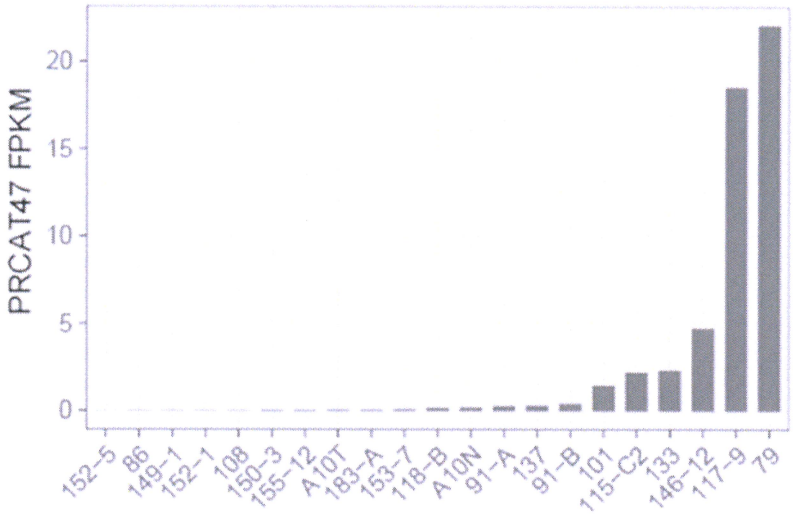

Figure 8: Expression of PRCAT47 in a panel of patient-derived xenografts of prostate cancer (measured by FPKM value from RNA-Seq analysis)

Although xenograft MDA-146-12 has the third highest expression of PRCAT47 among PDXs queried, qPCR analysis demonstrated that the expression level is still relatively low, compared to other AR-positive cell lines (MDA-PCa-2b, LNCaP, etc.) The result is demonstrated in Figure 9.

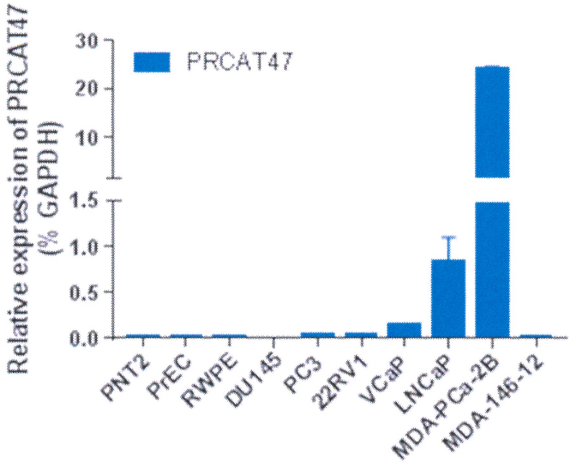

Figure 9: Expression of PRCAT47 across a panel of prostate cancer cells, and patient-derived xenograft MDA-146-12, measured by qPCR analysis.

(2) Evaluating *in-vivo* free-uptake efficacy of antisense oligonucleotides targeting PRCAT47.

As a first step to test *in-vivo* free-uptake efficacy, we initiated an *in vivo* study using MDA-146-12 patient derived xenograft. The experiment was approved by the University of Michigan

Institutional Animal Care and Use Committee (IACUC). Six to eight week old male athymic nude mice were inoculated subcutaneously with suspended cells from MDA-146-12 patient derived xenograft in the posterior dorsal flank region (5 million cells/site, two sites / animal). When the mean tumor volume reached approximately 150 mm^3, mice were randomized into two groups, respectively treated with PRCAT47-specific or control ASO. ASOs, dosed 50 mg/kg, were subcutaneously injected between the scapulae once daily for a week (five days on/two days off). Mice were then sacrificed and the primary tumors were excised for RNA extraction and ASO free-uptake evaluation (by qPCR analysis). Though expression level of PRCAT47 is not very high, we still observed a significant on-target effect of ASOs *in vivo*.

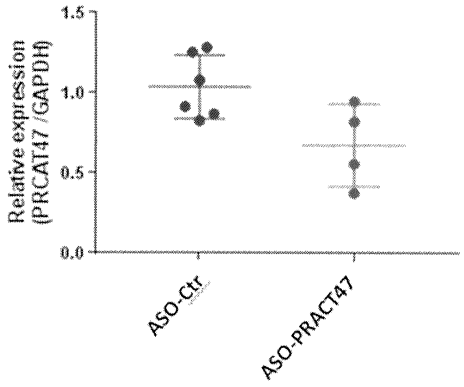

Figure 10: Relative expression of PRCAT47 in MDA-146-12 patient derived xenografts treated for control ASOs or ASO targeting PRCAT47, measured by qPCR analysis.

(3) Generation of cell-line derived xenograft in mice using MDA-PCa-2b cells.

To further test the *in-vivo* therapeutic effect of PRCAT47 ASOs, we tried to establish cell-line derived xenograft from MDA-PCa-2b cells. The experiment was approved by the University of Michigan Institutional Animal Care and Use Committee (IACUC). Six to eight week old male athymic nude mice were inoculated subcutaneously with MDA-PCa-2b cells suspended in matrigel scaffold in the posterior dorsal flank region (5 million cells/site, two sites /animal). When the mean tumor volume reached approximately 150 mm^3, mice were randomized into two groups, respectively treated with PRACT47-specific or control ASO. ASOs, dosed 50 mg/kg, were subcutaneously injected between the scapulae once daily for a week (five days on/two days off). Mice were then sacrificed and the primary tumors were excised for RNA extraction and ASO free-uptake efficacy evaluation (by qPCR analysis).

We observed a ~25% knockdown of PRCAT47 at the end of dosing period. And given the fact that this is the cell line-derived xenograft available with the highest PRCAT47 expression, we decided to perform tumor generation assay and ASO treatment using this xenograft during our next research cycle.

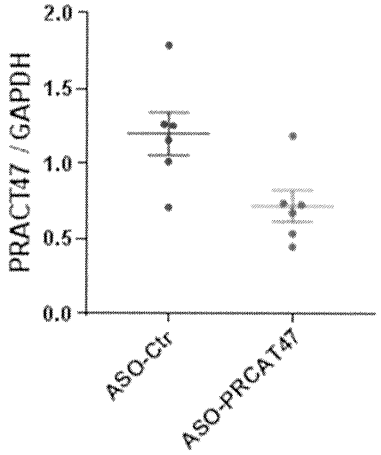

Figure 11: Relative expression of PRCAT47 in MDA-PCa-2b cell line derived xenografts, treated with control ASOs or ASO targeting PRCAT47, measured by qPCR analysis.

Impact

What was the impact on the development of the principle discipline(s) of the project?

At the end of the reported research cycle, we have finished ~70% of the proposed project, "Discovery and characterization of PRCAT47: A novel prostate lineage and cancer specific long non-coding RNA". The knowledge gained thus far has broadened our understanding of lncRNA functioning mechanisms. We delineated lncRNA as a possible node to regulate transcript stability. This function is partially mediated by lncRNA-protein interactions. We are now actively exploring the potential role of this lncRNA as a diagnostic marker and therapeutic target in prostate cancer. We anticipate that at the end of this project, we will be able to determine whether PRCAT47 represents a novel node in targeting AR signaling, and whether targeting lncRNAs by antisense technologies serves as an efficient approach to inhibit pathogenic lncRNAs in cancer context.

What was the impact on other disciplines?

Nothing to report

What was the impact on technology transfer?

Nothing to report

What was the impact on society beyond science and technology?

Nothing to report

Changes/Problems

Changes in approach and reasons for change:

We did not propose to perform BrU-Seq and BrUChase-Seq to study transcript stability in our initial proposal. We added this experiment because this technique allowed a more accurate profiling of transcript synthesis rate and degradation rate. Without this assay, we could not pinpoint the specific steps changed (synthesis or degradation) in the life cycle of a transcript.

Products

Nothing to report

Participants & Other Collaborating Organizations

Name:	Rohit Mehra
Project Role:	Principal Investigator
Researcher Identifier (e.g. ORCID ID):	0000-0002-6955-8884
Nearest person month worked:	1.0
Contribution to Project:	Dr. Mehra has supervised proposed research and study personnel, drafted experiments, constructed tissue microarrays (TMAs) from various clinical cohorts of patients with localized and metastatic prostate cancer, performed and optimized RNA in situ Hybridization (RNA-ISH).
Funding Support:	DOD

Name:	Yajia Zhang

Project Role:	Ph.D. candidate
Researcher Identifier (e.g. ORCID ID):	
Nearest person month worked:	
Contribution to Project:	Ms. Zhang performed various functional studies as well as molecular biology experiments.
Funding Support:	DoD Fellowship

Name:	Lisha Wang
Project Role:	Research fellow
Researcher Identifier (e.g. ORCID ID):	
Nearest person month worked:	
Contribution to Project:	Dr. Wang assisted in the development of the RNA-ISH assay.
Funding Support:	

Name:	Pankaj Vats
Project Role:	Bioinformatic Analysis
Researcher Identifier (e.g. ORCID ID):	

Nearest person month worked:	1.0
Contribution to Project:	Mr. Vats assisted in the analysis of the high throughput data including RIP-Seq and ChIRP-seq
Funding Support:	

Name:	Xia Jiang
Project Role:	Technician
Researcher Identifier (e.g. ORCID ID):	
Nearest person month worked:	3
Contribution to Project:	Ms. Jiang performed cell culture, various functional studies as well as molecular biology experiments.
Funding Support:	

Special Reporting Requirements

Nothing to report

Abbreviations

CRPC, castration-resistant prostate cancer
AR, Androgen Receptor
ADT, Androgen deprivation therapies
LncRNA, long non-coding RNA

References

1 Iyer, M. K. *et al.* The landscape of long noncoding RNAs in the human transcriptome. *Nat Genet* **47**, 199-208, doi:10.1038/ng.3192 (2015).
2 Siegel, R. L., Miller, K. D. & Jemal, A. Cancer statistics, 2018. *CA: a cancer journal for clinicians* **68**, 7-30, doi:10.3322/caac.21442 (2018).
3 Lu-Yao, G. L. *et al.* Fifteen-year survival outcomes following primary androgen-deprivation therapy for localized prostate cancer. *JAMA Intern Med* **174**, 1460-1467, doi:10.1001/jamainternmed.2014.3028 (2014).
4 Wong, Y. N., Ferraldeschi, R., Attard, G. & de Bono, J. Evolution of androgen receptor targeted therapy for advanced prostate cancer. *Nat Rev Clin Oncol* **11**, 365-376, doi:10.1038/nrclinonc.2014.72 (2014).
5 Scher, H. I. *et al.* Increased survival with enzalutamide in prostate cancer after chemotherapy. *N Engl J Med* **367**, 1187-1197, doi:10.1056/NEJMoa1207506 (2012).
6 Watson, P. A., Arora, V. K. & Sawyers, C. L. Emerging mechanisms of resistance to androgen receptor inhibitors in prostate cancer. *Nat Rev Cancer* **15**, 701-711, doi:10.1038/nrc4016 (2015).
7 Antonarakis, E. S. *et al.* AR-V7 and resistance to enzalutamide and abiraterone in prostate cancer. *N Engl J Med* **371**, 1028-1038, doi:10.1056/NEJMoa1315815 (2014).
8 Hearn, J. W. D. *et al.* HSD3B1 and resistance to androgen-deprivation therapy in prostate cancer: a retrospective, multicohort study. *The Lancet. Oncology* **17**, 1435-1444, doi:10.1016/S1470-2045(16)30227-3 (2016).
9 Yeap, B. B. *et al.* Novel binding of HuR and poly(C)-binding protein to a conserved UC-rich motif within the 3'-untranslated region of the androgen receptor messenger RNA. *J Biol Chem* **277**, 27183-27192, doi:10.1074/jbc.M202883200 (2002).
10 Paulsen, M. T. *et al.* Use of Bru-Seq and BruChase-Seq for genome-wide assessment of the synthesis and stability of RNA. *Methods* **67**, 45-54, doi:10.1016/j.ymeth.2013.08.015 (2014).